Journal of the European Ceramic Society 20 (2000) 2095–2100

Diffusion of calcium in yttria stabilized zirconia ceramics

K. Kowalski [a,*], A. Bernasik [a], A. Sadowski [b]

[a] *Surface Spectroscopy Laboratory, University of Mining and Metallurgy and Joint Centre for Chemical Analysis and Structural Research, Jagellonian University, ul. Reymonta 23, Kraków, Poland*
[b] *University of Mining and Metallurgy, al. Mickiewicza 30, Kraków, Poland*

Received 27 November 1999; received in revised form 13 March 2000; accepted 25 March 2000

Abstract

Bulk and grain boundary diffusion of calcium in yttria fully stabilized zirconia was studied in air in the temperature range from 1100 to 1400°C. Secondary ion mass spectrometry (SIMS) was used to determine the diffusion profiles as average concentration vs. depth in the B-type kinetic region. The obtained results allowed the calculation of the temperature dependence of the bulk diffusion coefficient D and the grain boundary diffusion parameter $D'\delta s$. Activation energies of these processes amount to 333 and 367 kJ mol^{-1}, respectively. Diffusion data of calcium were compared to those of titanium obtained previously using the same zirconia material.

Keywords: Diffusion; Grain boundaries; ZrO_2

1. Introduction

Transport properties of cation sub-lattice in stabilized zirconia, especially the diffusion along grain boundaries, are still not well known. The reported data, dealing mainly with bulk diffusion, are scarce and not systematic. Review of the results, concerning the cation diffusion, as well as of the applied experimental methods, has been presented in a previous paper.[1] It has been shown that only a few experiments were performed.[2–7] Furthermore, they were done on materials stabilized with different types and amounts of stabilizers. Various experimental techniques used in these investigations were mostly indirect methods of determination of the diffusion parameters. The grain boundary transport was studied by Oishi et al.[3–5] in some interdiffusion experiments. The authors of the present work investigated the bulk and grain boundary diffusion of titanium[1] in yttria fully stabilized zirconia using secondary ion mass spectrometry (SIMS). In a recent work by Matsuda et al.[8] the bulk and grain boundary diffusion of calcium in yttria stabilized zirconia was studied also by SIMS.

This technique appeared to be a powerful tool for studying the transport processes in ceramics in the temperature range where diffusion distances are too small to be analysed by serial mechanical sectioning. This was a simple and reliable method for direct determination of the diffusion parameters.[1]

The present work is an attempt to determine the transport properties of calcium in the yttria fully stabilized zirconia. As in the previous study,[1] the zirconia material and the experimental technique were the same. This enabled direct comparison of the diffusion parameters of Ca^{2+} and Ti^{4+} ions differing in valency and radius. The calcium diffusion results were also compared with the literature data on the diffusion of calcium in other stabilized zirconia systems.

2. Theoretical background

The diffusion experiments were performed in the B-type kinetic regime[9–11] valid when

$$s\delta \ll (Dt)^{1/2} \ll g \tag{1}$$

where D denotes bulk diffusion coefficient, t time, s segregation factor of the tracer diffusing in grain boundaries defined as the ratio between the grain boundary and

* Corresponding author. Tel.: +48-12-617-2716; fax: +48-12-634-3070.
E-mail address: kowalski@zawrat.metal.agh.edu.pl (K. Kowalski).

0955-2219/00/$ - see front matter
PII: S0955-2219(00)00103-5

bulk concentrations of the tracer, δ grain boundary width and g grain size.

The condition expressed by Eq. (1) means that the penetration distance in the bulk, defined as $(Dt)^{1/2}$, is much deeper than the grain boundary width and much shorter than the grain size. If the tracer, before annealing, is deposited on the surface then the transport process consists of three diffusion ways: the first one—from the surface to the volume of the adjacent grains, the second one—along the grain boundaries and the third one—from the grain boundaries to the neighbouring grains. The mean penetration distance $(Dt)^{1/2}$ in the bulk is so small that the tracer fluxes coming from different grain boundaries do not overlap and thus the grain boundaries can be considered as isolated.[9–11]

Usually, the bulk diffusion coefficient D is much lower (often several orders of magnitude) than the grain boundary one, D'. Therefore, the diffusion profile in the region B, expressed as mean concentration of the tracer vs. depth, consists of two parts.[9–11] The first one, characterised by high slope, is a result of the diffusion from the sample surface to the bulk of grains. It is possible to calculate the bulk diffusion coefficient from this part of the profile according to the following equation, which is valid for very thin initial layer of the tracer:

$$D = -\left(4 \cdot t \cdot \frac{\partial \ln \bar{c}}{\partial x^2}\right)^{-1} \tag{2}$$

where $\bar{c}$ is average concentration in a very thin slice parallel to the surface and x is depth.

The second part of the concentration profile, characterised by a much lower slope, represents the diffusion from grain boundaries into the grains. This part of the profile enables to calculate the product $D'\delta s$, according to the equation:

$$D'\delta s = 0.66 \cdot \left(-\frac{\partial \ln \bar{c}}{\partial x^{6/5}}\right)^{-5/3} \cdot \left(\frac{4D}{t}\right)^{1/2} \tag{3}$$

3. Experimental

The samples of yttria stabilized zirconia of nominal composition 92 mol% ZrO_2–8 mol% Y_2O_3 were prepared by sintering fine-grained (0.3 μm) powder compacts at 1700°C for 2 h in air. The powder was prepared by co-precipitation of $ZrOCl_2$ and YCl_3 solutions, and subsequent calcination and milling. The powder compacts were formed by uniaxial pressing at 100 MPa followed by isostatic pressing at 300 MPa. Finally, the samples had the form of round pellets, 10 mm in diameter and 2 mm thick.

The obtained zirconia specimens were compact with densities higher than 99% of the theoretical ones and consisted of grains with an average diameter of 15 μm. Total amount of impurities did not exceed 0.1 wt.% (Table 1). Crystallographic structure of the investigated material was verified by X-ray diffraction measurements (XRD). The samples contained cubic phase only.

One drop of a saturated solution of calcium nitrate, was deposited on the polished surface of the samples at room temperature. Then, the samples were dried in air up to temperature 200°C for 2 h. The obtained layer was thin but rough. Therefore, prior to diffusion annealings the samples were softly polished. Due to small thickness of the deposited layer we considered it as an instantaneous source of a tracer during the diffusion process.

The diffusion annealings were done in air at 1100, 1150, 1200, 1300, 1350 and 1400°C for 68, 47, 24, 6, 6 and 2 h, respectively. In these conditions Eq. (1) was fulfilled. No further sintering or grain size variations were observed.

SIMS in-depth profiles were determined under the pressure less than 10^{-8} mbar. Double lens liquid metal ion beam gun (by FEI Company) was used to sputter the area of about 100 μm × 100 μm with Ga^+ primary ion beam, with the energy of 25 keV and the current of 2 nA. Secondary ions were detected in the Balzers quadrupole mass spectrometer. Undesirable edge effects were avoided by analysing, exclusively, the ions coming from the central 40% of the crater area, using an electronic gate. Charging effects on sputtering and analysis were eliminated by applying the electron flood gun, with the energy of about 250 eV. The crater dimensions were sufficient to analyse at least several grains and boundaries between them. Depths of the sputtered craters were measured with a profilometer. They were usually in the range between 1.5 and 2 μm. The measured crater depths and the time of sputtering were used to calibrate the depth axis of the profiles. The depth inaccuracy resulting from the roughness of the crater bottom was about 8%.

Diffusional profiles were determined by measuring the signal intensities of four isotopes: ^{40}Ca, ^{89}Y, ^{90}Zr and ^{94}Zr on sputtering. As the crater area was large compared to

Table 1
Impurity content in studied zirconia

Element	Si	Fe	Mn	Mg	Al	Ti	Ge, Pt, Ta, Au, Mo, W, Ni, V, Sn, Pb
wt.%	0.054	0.030	0.0025	0.015	0.0012	0.001	not found

the grain size, these intensities were proportional to the mean concentration of monitored isotopes at a given depth resulting from the sputtering time. Three hours were usually sufficient to obtain a complete diffusion profile. The measurements were repeated several times in different areas on the same sample.

4. Results and discussion

SIMS profiles were analysed as a function of intensity ratios: $^{40}Ca/^{90}Zr$, $^{89}Y/^{90}Zr$ and $^{94}Zr/^{90}Zr$ vs. depth. This method allowed the elimination of the effect of possible small variations of ion current on long-term sputtering. The constant ratio of yttrium and zirconium isotope intensities: $^{89}Y/^{90}Zr$ and $^{94}Zr/^{90}Zr$, resulting from constant bulk concentrations of these isotopes in the investigated zirconia, was a criterion of the measurement correctness.

One of the obtained diffusion profiles is shown in Fig. 1. This profile was taken from a specimen annealed at 1150°C for 47 h. The ratios of the signal intensities of yttrium and zirconium isotopes are independent of depth. The $^{40}Ca/^{90}Zr$ intensity ratio curve exhibits two well-distinguished parts, characteristic of the B-type kinetic. Fig. 1 illustrates also the way of determination of the bulk and grain boundary diffusion parameters from the two parts of the profile according to Eqs. (2) and (3).

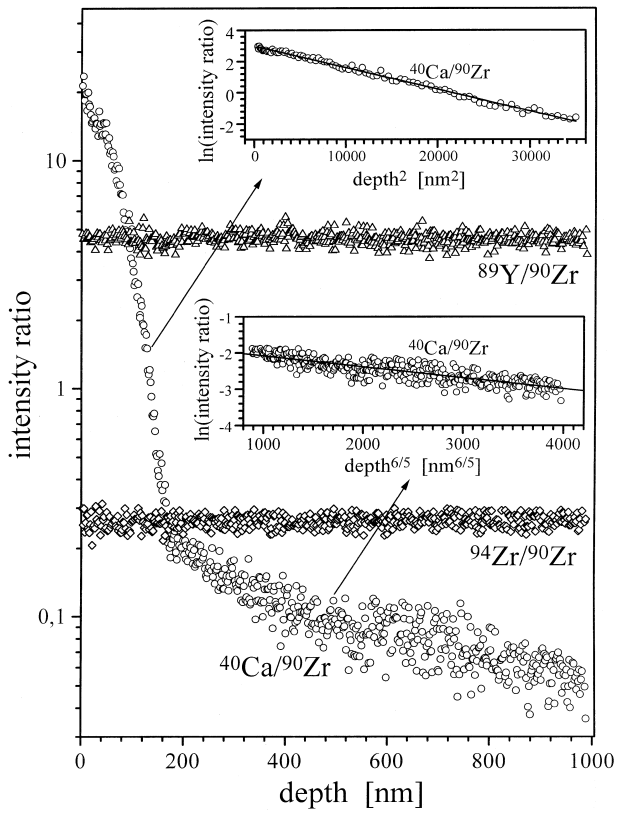

Fig. 1. Diffusion depth profile for the sample annealed at 1150°C for 47 h.

The shape of the diffusion profile is not a sufficient criterion for the determination of the transport process. The obtained shapes, even if characteristic of the B-type kinetics, should correspond to the distribution of calcium caused by the bulk and grain boundary diffusion and not by other effects or artefacts. Therefore, additional SIMS measurements were performed in order to determine 2-dimensional distribution of Ca vs. depth. Fig. 2 shows a map illustrating the distribution of calcium (^{40}Ca) at the depth of 300 nm in a sample annealed at 1150°C for 47 h. As follows from Fig. 1, at this depth the average concentration of calcium should depend mainly on the transport from grain boundaries to the bulk. This assumption seems to be correct because, as can be seen in Fig. 2, calcium is concentrated along the grain boundaries only.

Bulk diffusion coefficient D and grain boundary diffusion parameter $D'\delta s$ obtained in this work are shown in Fig. 3 in the Arrhenius plot. The temperature dependences of the bulk diffusion coefficient and the grain boundary diffusion parameter can be described by the following equations:

$$D = 3.5(\pm 7.0)\cdot 10^{-7} \cdot \exp\left(\frac{-333(\pm 25)\ \mathrm{kJ\,mol^{-1}}}{RT}\right)[\mathrm{m^2 s^{-1}}] \quad (4)$$

$$D'\delta s = 5.9(\pm 21.3)\cdot 10^{-10} \cdot \exp\left(\frac{-367(\pm 46)\ \mathrm{kJ\,mol^{-1}}}{RT}\right)[\mathrm{m^3 s^{-1}}] \quad (5)$$

where T is absolute temperature of annealing and R is the gas constant.

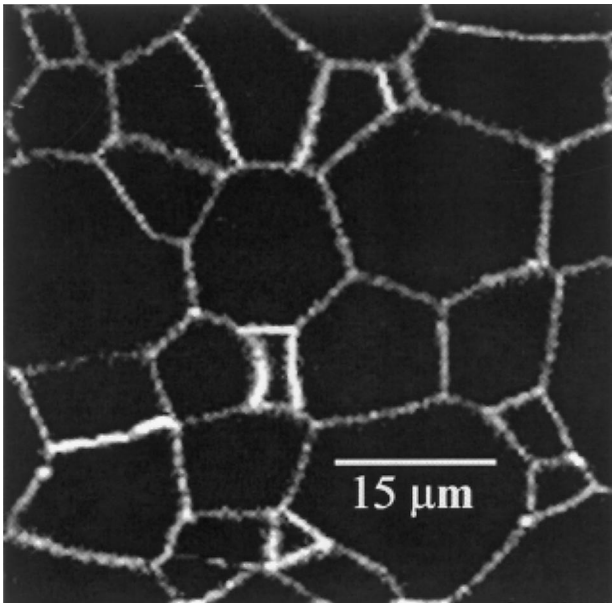

Fig. 2. Distribution of calcium in thin slice parallel to the surface at depth of 300 nm determined for the sample annealed at 1150°C for 47 h.

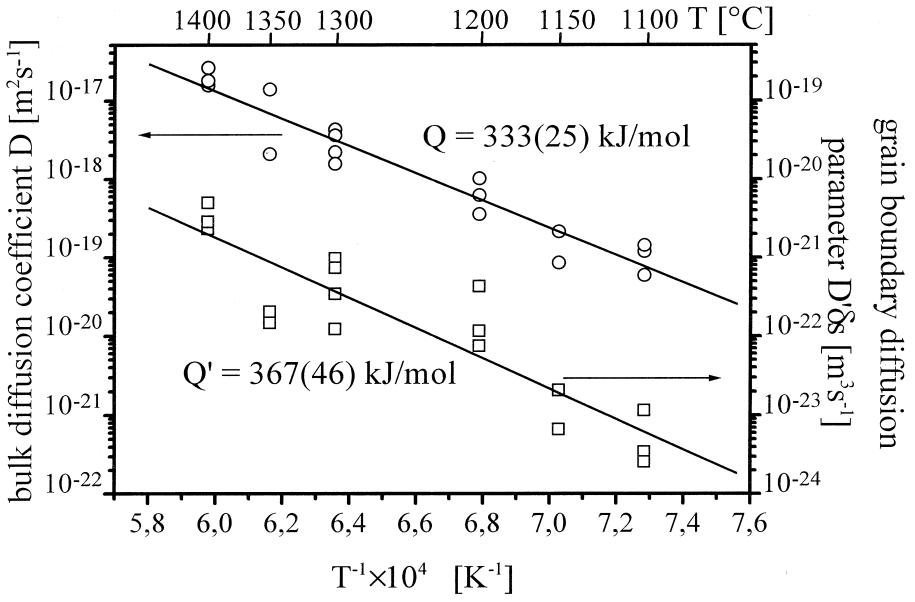

Fig. 3. Arrhenius plot of the diffusion parameters.

Values in brackets are standard deviations of the calculated values.

Diffusion data obtained in this study and in the previous works are shown in Fig. 4 for the bulk diffusion and in Fig. 5 for the grain boundary diffusion. Description of curves, presented in Figs. 4 and 5, which comprises chemical composition of the used zirconia samples and the investigated transport processes, is presented in Table 2.

The present results have been obtained using the same experimental method and material as in the previous work[1] on the diffusion of titanium. Thus, they could be compared directly. The activation energy of Ti bulk diffusion, equal to 505(±32) kJ mol^{-1}, is greater than that of Ca: 333(±25) kJ mol^{-1}. Contrary to this, the activation energy of grain boundary diffusion, in the range of experimental error, is almost the same, 340(±49) and 367(±46) kJ mol^{-1} for Ti and Ca, respectively. Finally, the ratio of activation energies of bulk diffusion and grain boundary diffusion was 1.10(±0.22) for Ca and 0.67(±0.12) for Ti.

The results obtained by Oishi et al. at higher temperatures showed that the ratio of activation energies of bulk and grain boundary Hf-Zr interdiffusion in a 16 mol% CaO–$(Zr_{1-x}Hf_x)O_2$ system[3] was 0.68 and in a 16 mol% Y_2O_3–$(Zr_{1-x}Hf_x)O_2$ system[4] it was 0.78. For the Ca–Zr interdiffusion in the 13 and 19 mol% CaO–ZrO_2 coupled specimens[5] this ratio was equal to 0.98. Thus comparison of the data by Oishi et al.[3–6] with the results of our works on Ti and Ca diffusion in the 8 mol% Y_2O_3–ZrO_2 system indicates that for the diffusing ions with similar ionic radii: Ti^{4+} and Hf^{4+}, this ratio is almost the same and distinctly less than 1. Ti^{4+} and Hf^{4+} have the ionic radii of 0.068 and 0.083 nm respectively,[12] which are smaller and close to the radius

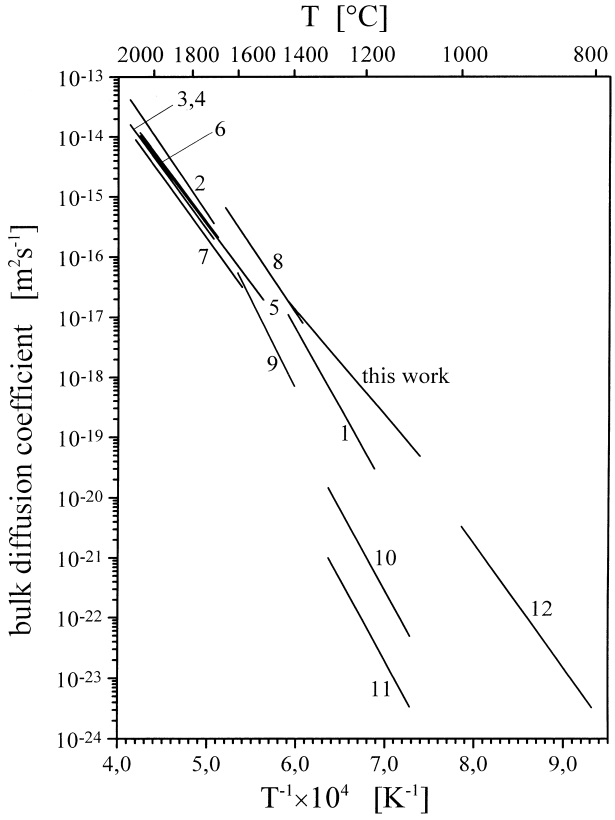

Fig. 4. Bulk diffusion coefficients D in fully stabilized zirconia systems obtained by different authors. Description of curves in Table 2.

of the Zr^{4+} ion (0.084 nm). For the diffusion of the greater ion Ca^{2+} (0.112 nm) the ratio is close to 1. This is inconsistent with the result obtained by Matsuda et al.[8] for the diffusion of calcium in 10 mol% Y_2O_3–ZrO_2 at lower temperatures. They found this ratio equal to

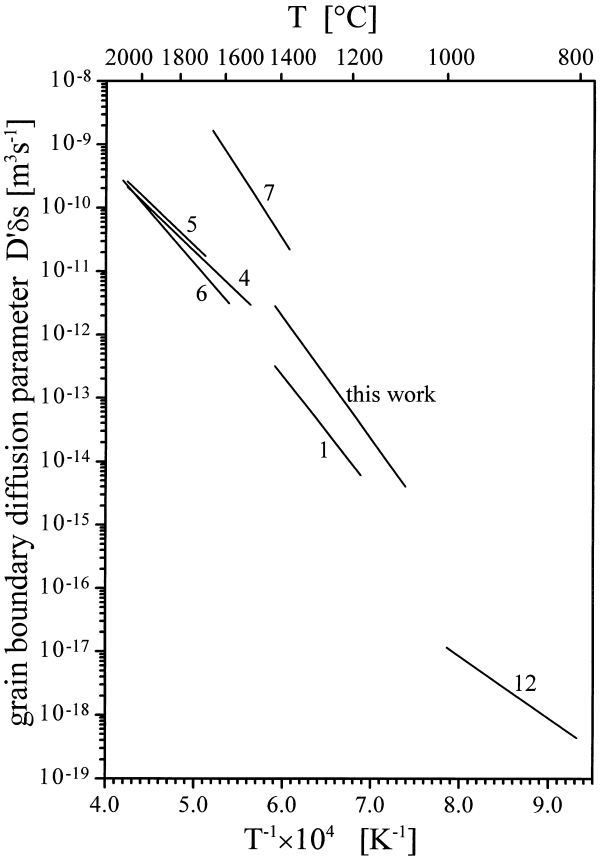

Fig. 5. Grain boundary diffusion parameters $D'\delta s$ in fully stabilized zirconia systems obtained by different authors. Description of curves in Table 2.

0.47. Such a low value resulted from a much lower activation energy of grain boundary transport—185 kJ mol^{-1} as the activation energy of bulk diffusion was similar. However, it must be noticed that the scatter of experimental points by Matsuda et al. used for the calculation of the activation energy of grain boundary diffusion was much greater than that presented by Oishi et al. and that in our works.

In the literature[13] it is usually assumed that if the mechanism of diffusion in bulk and along grain boundaries is the same, then the activation energy of grain boundary diffusion is about 2/3 of the activation energy of bulk diffusion. This results from a less-packed and highly defected structure of grain boundaries compared to the bulk. Such a situation is met in pure metals and in the majority of studied oxides.[1,13] However, if the segregation of impurities to grain boundaries is very strong and saturation effects appear, then further considering the grain boundaries as the same material as the bulk, only more defected, is no longer valid. New phases can be found in grain boundaries and simple comparison of diffusion mechanisms in the bulk and in the grain boundaries is groundless. It has been found in certain oxides[13] that the activation energy ratio is higher than 1 and this fact can be explained by a different diffusion mechanism in grain boundaries or/and different grain boundary composition.

In fact, it is now well known from the grain boundary segregation studies[14,15] and electric a.c. conductivity measurements[15–17] that grain boundaries of the stabilized zirconia can contain glassy oxide phases induced by segregation (or co-segregation) of impurities, mainly silicon, aluminium, iron and others. This effect occurs even in very pure zirconia materials and is dependent on grain size, sintering conditions, history of a specimen and obviously on the bulk content of impurities. Consequently, the physical properties of grain boundaries, such as electrical conductivity and mass transport, strongly depend on their chemical composition and structure. This leads to the situation where zirconia materials of the same nominal composition, obtained by different authors, may have similar bulk properties but quite different properties of grain boundaries. From this point of view, reliable conclusions concerning the grain boundary diffusion mechanisms can be drawn exclusively from the experimental data obtained for the same material. At present the available data are not sufficient for this purpose.

Table 2
Description of curves presented in Figs. 4 and 5

Curve number	Composition of zirconia	Transport process	Reference
1	8 Mol% Y_2O_3–ZrO_2	Ti diffusion	1
2	16 Mol% CaO–ZrO_2	^{45}Ca diffusion	2
3	16 Mol% CaO–ZrO_2	^{95}Zr diffusion	2
4	12 Mol% CaO–ZrO_2	As above	2
5	16 Mol% CaO–$(Zr_{1-x}Hf_x)O_2$ $x_1=0.020$, $x_2=0.100$	Interdiffusion Zr–Hf	3
6	14 Mol% MgO - $(Zr_{1-x}Hf_x)O_2$ $x_1=0.020$, $x_2=0.100$	As above	3
7	16 Mol% Y_2O_3 - $(Zr_{1-x}Hf_x)O_2$ $x_1=0.020$, $x_2=0.100$	As above	4
8	13 Mol% CaO–ZrO_2 19 mol% CaO–ZrO_2	Interdiffusion Ca–Zr	5
9	25 Mol% Y_2O_3–ZrO_2	Effective lattice diffusivity in diffusional creep	6
10	9.4 Mol% Y_2O_3–ZrO_2 single crystal	Zr vacancy diffusion in a dislocation loop shrinkage	7
11	18 Mol% Y_2O_3–ZrO_2 single crystal	As above	7
12	10 Mol% Y_2O_3–ZrO_2	Ca diffusion	8

5. Conclusions

Comparison of the diffusion data of titanium and calcium for the same zirconia material and applied experimental method, showed that while the activation energy of bulk diffusion of Ti (505 kJ mol^{-1}) is distinctly higher than that obtained for Ca (333 kJ mol^{-1}), the activation energy of grain boundary diffusion is practically the same (340 and 367 kJ mol^{-1}, respectively).

The ratio of activation energies of bulk diffusion and grain boundary diffusion of Ti (0.67) is very close to that obtained by Oishi et al.[3,4] for the Hf–Zr interdiffusion measurements. In the case of Ca diffusion, this ratio obtained in the present work and in the Ca–Zr interdiffusion experiments by Oishi et al.[5] is almost the same, close to 1.

Thorough understanding of the grain boundary diffusion mechanism in a stabilized zirconia calls for further studies using the same material.

Acknowledgements

This work was supported by the Polish State Committee for Scientific Research under Grant No 7T08A 001 10 during the years 1996-1999. The authors are very grateful to Prof. K. Haberko and Dr. W. Pyda for providing the zirconia materials.

References

1. Kowalski, K., Bernasik, A. and Sadowski, A., Bulk and grain boundary diffusion of titanium in yttria stabilized zirconia. *J. Eur. Ceram. Soc.*, 2000, **20**(7), 951–958.
2. Rhodes, W. H. and Carter, R. E., Cationic self-diffusion in calcia-stabilized zirconia. *J. Am. Ceram. Soc.*, 1966, **49**(5), 244–249.
3. Oishi, Y., Sakka, Y. and Ando, K., Cation interdiffusion in polycrystalline fluorite-cubic solid solutions. *J. Nucl. Mater.*, 1981, **96**, 23–28.
4. Sakka, Y., Oishi, Y. and Ando, K., Zr-Hf interdiffusion in polycrystalline Y_2O_3-$(Zr+Hf)O_2$. *J. Mater. Sci.*, 1982, **17**, 3101–3105.
5. Oishi, Y. and Ichimura, H., Grain-boundary enhanced interdiffusion in polycrystalline CaO-stabilized zirconia systems. *J. Chem. Phys*, 1979, **71**(12), 5134–5139.
6. Dimos, D. and Kohlstedt, D. L., Diffusional creep and kinetic demixing in yttria-stabilized zirconia. *J. Am. Ceram. Soc.*, 1987, **70**(8), 531–536.
7. Chien, F. R. and Heuer, A. H., Lattice diffusion kinetics in Y_2O_3-stabilized cubic ZrO_2 single crystals: a dislocation loop annealing study. *Phil. Mag. A*, 1996, **73**(3), 681–697.
8. Matsuda, M., Nowotny, J., Zhang, Z. and Sorell, C. C., Lattice and grain boundary diffusion of Ca in polycrystalline yttria-stabilized ZrO_2 determined by employing SIMS technique. *Solid State Ionics*, 1998, **111**, 301–306.
9. Kaur, I., Gust, W.. Fundamentals of grain and interface boundary diffusion, Stuttgart; Ziegler Press, 1988.
10. Mishin, Y., Herzig, C. and Bernardini, J. and Gust, W., Grain boundary diffusion: fundamentals to recent developments. *Int. Met. Rev.*, 1997, **42**(4), 155–178.
11. Mishin, Y. and Herzig, C., Grain boundary diffusion: recent progress and future research. *Mater. Sci. Eng.*, 1999, **A260**, 55–71.
12. Evans, H. T., Jr., Ionic radii in crystals. In *Handbook of Chemistry and Physics, A Ready-Reference Book of Chemical and Physical Data*, ed. D.R. Lide. 76th ed. CRC Press, Boca Raton, New York, London, Tokyo, 1995–1996, pp. 12-4–12-15.
13. Monty, C. and Atkinson, A., Grain-boundary mass transport in ceramic oxides. *Cryst Latt. and Amorph. Mat*, 1989, **18**, 97–120.
14. Hughes, A. E. and Sexton, B. A., XPS study of an intergranular phase in yttria-zirconia. *J. Mater. Sci.*, 1989, **24**, 1057–1061.
15. Aoki, M., Chiang, Y.-M., Kosacki, I., Lee, L. J.-R., Tuller, H. and Liu, Y., Solute segregation and grain boundary impedance in high-purity stabilized zirconia. *J. Am. Ceram. Soc.*, 1996, **79**(5), 1169–1180.
16. Badwal, S. P. S. and Drennan, J., Yttria-zirconia: effect of microstructure on conductivity. *J. Mater. Sci.*, 1987, **22**, 3231–3239.
17. Guo, X., Solute segregations at the space-charge layers of stabilized zirconia: an opportunity for amelorating conductivity. *J. Eur. Ceram. Soc.*, 1996, **16**, 575–578.